Synthesis and Multidimensional NMR Characterization of PDMS-*b*-PS Prepared by Combined Anionic Ring-Opening and Nitroxide-Mediated Radical Polymerization

Andre' M. Morgan,† Steven K. Pollack,*,† and Kebede Beshah‡

Department of Chemistry and the Polymer Science and Engineering Program, Howard University, Washington, D.C. 20059, and Rohm and Haas Research Laboratories, 727 Norristown Road, Spring House, Pennsylvania 19477

Received August 7, 2001; Revised Manuscript Received March 13, 2002

ABSTRACT: The synthesis of PDMS-*b*-PS copolymers by anionic and nitroxide-mediated radical polymerization (NMRP) is discussed. Hydride end-capped PDMS is hydrosilylated with an allylic alkoxyamine to form a TEMPO functional macroinitiator. The macroinitiator is reacted with styrene to form diblock copolymer. NMRP of styrene initiated by the PDMS macroinitiator ($M_w/M_n = 1.22$) gave diblocks with M_w/M_n between 1.28 and 1.35. Microstructure characterization by one (1D) and two (2D) dimensional solution NMR verified the composition of the copolymer end groups and block junction. LC-NMR analysis shows that nearly homopolymer free diblocks were obtained by this method. Solid-state NMR analysis verified a phase-separated morphology.

Introduction

Poly(dimethylsiloxane)-*b*-polystyrene copolymers have been of scientific and technological interest for many years.[1] Composed of monomers with extremely different characteristics, these materials exhibit interesting properties, making them desirable engineering and commodity materials. The unique properties of PDMS-*b*-PS copolymers are mainly due to the presence of the inorganic, polysiloxane sequence. Some of the notable properties of siloxane polymers are high flexibility, causing them to have very low glass transition temperatures (T_g), low surface tension and surface energy, high gas permeability, and chemical and physiological inertness. Organic−siloxane copolymers such as PDMS-*b*-PS have potential uses as thermoplastic elastomers, compatibiizers, or surfactants in polymer blends. PDMS/PS block and graft copolymers have been incorporated into contact lenses, gas permeable films and tubes, release surfaces for pressure-sensitive adhesives, and lithographic printing masters.[2] PDMS/PS block copolymers have also been used as steric stabilizers during dispersion polymerization of styrene in supercritical CO_2.[3]

Poly(dimethylsiloxane)-*b*-polystyrene copolymers are traditionally synthesized by "living" anionic polymerization.[4−6,8−10] More than 30 years ago, Saam et al.[4] described the sequential anionic polymerization of styrene and hexamethylcyclotrisiloxane (D_3), using an alkyllithium initiator. Since then, others have gone on to synthesize multiple block and graft copolymers of PDMS and PS via anionic polymerization.[6,7,10,11] While anionic polymerization is successful, it does have some limitations. In general, anionic polymerization is limited by its applicability to a small number of monomers and incompatibility with desired polymer end groups. Also, reaction conditions call for the strict exclusion of impurities, such as moisture, oxygen, and CO_2. Because of these requirements, laboratory synthesis is performed using specially designed apparatuses and high-vacuum techniques in order to obtain well-defined copolymers.[11−13] Also, highly purified monomers and solvents must be used, which are expensive for large-scale production. Because of these disadvantages, producing PDMS-*b*-PS, and other copolymers synthesized by anionic polymerization, by alternative methods is of current interest.[14]

Recently, there has been a burst of activity in an alternative method of living polymerization called controlled ("living") radical polymerization. Several types of controlled radical polymerization techniques have been introduced: nitroxide-mediated radical polymerization (NMRP), atom transfer radical polymerization (ATRP), and reversible addition−fragmentation chain transfer polymerization (RAFT).[14,15] NMRP is of interest in this paper. NMRP involves using a nitroxide, such as 2,2,6,6-teteramethylpiperidinyl-1-oxy (TEMPO), to mediate the polymerization of vinyl monomers. Moad and Rizzardo introduce the use of TEMPO for controlled radical polymerization.[16] The goal of synthesizing narrowly dispersed polymer using the nitroxide remained elusive until a procedure reported by Georges et al.[17] This group synthesized polystyrene using a bimolecular mixture of benzoyl peroxide and TEMPO, resulting in polymer with a polydispersity < 1.3. Craig Hawker developed this method even further by synthesizing a unimer, **1**, by a similar technique. He then used this

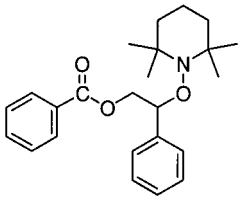

1

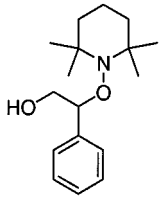

2

unimer to synthesis controlled molecular weight, narrowly dispersed polymer. Compound **1**, containing only one reactive moiety, was later modified to produce the

† Howard University.
‡ Rohm and Haas Research Laboratories.

10.1021/ma0114178 CCC: $22.00
Published on Web 04/24/2002

Scheme 1

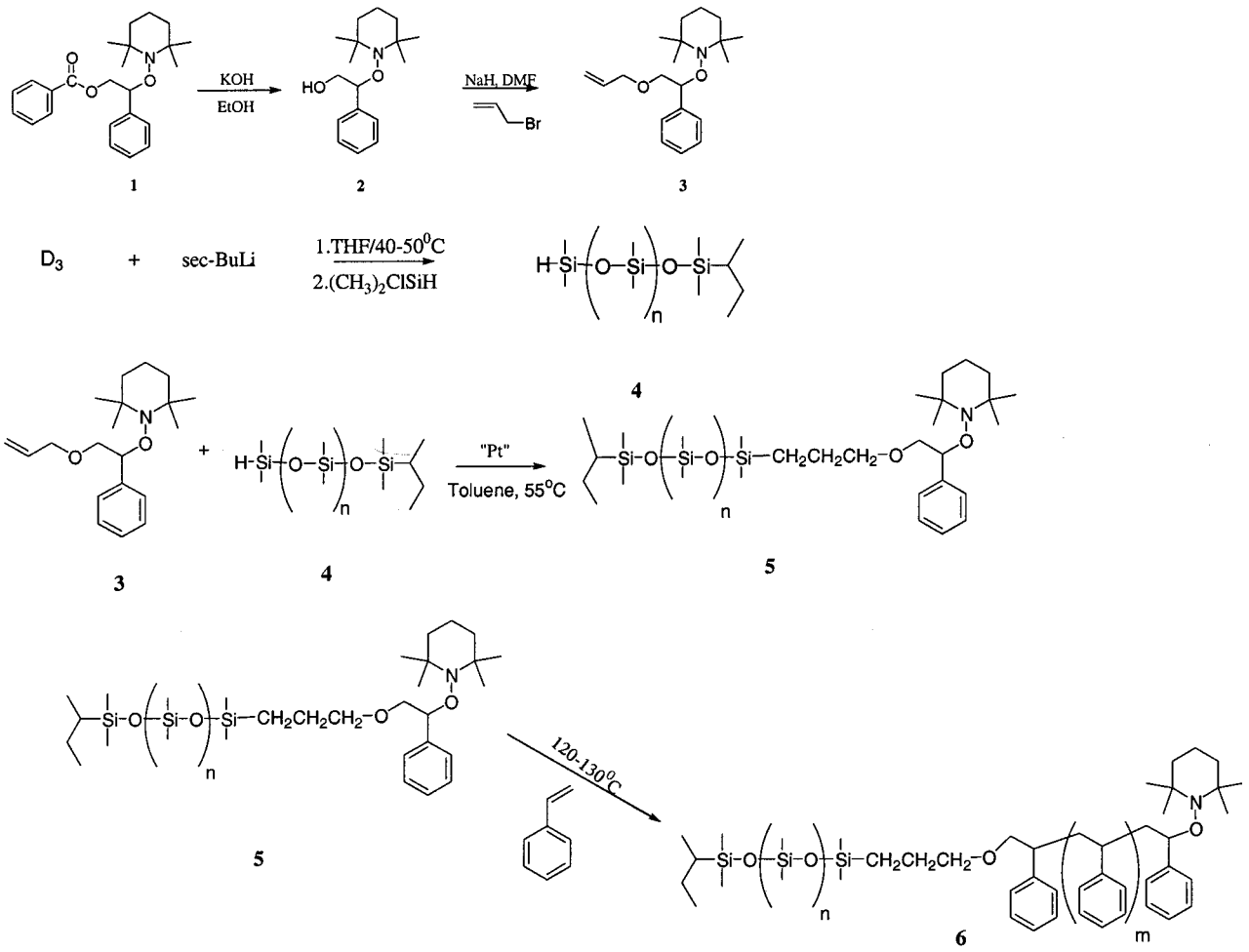

difunctional initiator, **2**.[18] Kobatake et al.[19] used **2** to synthesize a nitroxy-functionalized polybutadiene macroinitiator. This macroinitiator was then used for polymerization of styrene via NMRP, resulting in polybutadiene-*b*-polystyrene copolymer.[20] A variety of multifunctional initiators such as **2** have since been used to create block and graft copolymers by a hybrid of NMRP with other polymerization techniques (anionic, cationic, condensation, etc.).[14,21−27] Although one step in the synthesis may still involve ionic polymerization, improved control over molecular design may be gained using a two-step process.

Two groups have previously described combined "living" anionic and NMRP of poly(dimethylsiloxane)-*b*-polystyrene. Yoshida and Tanimoto used a PDMS macroinitiator, containing an azo moiety, with MTEMPO (4-methoxy-2,2,6,6-tetramethylpiperidine-1-oxy) to form PDMS-*b*-PS, having MTEMPO as one of the end groups.[26] Miura and co-workers used a difunctional alkoxyamine, 4-lithiophenylalkoxyamine, to initiate anionic ring-opening polymerization of hexamethylcyclotrisiloxane, followed by NMRP of styrene to form the diblock.[28] While not in the scope of this text, PDMS/PS block and graft copolymers have also been synthesized by ATRP, using benzyl chloride terminated PDMS to initiate styrene polymerization.[29]

We have now added to the list of methods used to synthesize poly(dimethylsiloxane)-*b*-poly(styrene) copolymers (see Scheme 1). Starting with a difunctional allyl ether derivative of the alkoxyamine **2**, we have synthesized diblock copolymers of PDMS-*b*-PS via anionic ring-opening polymerization and nitroxide-mediated radical polymerization (Scheme 1). Thorough characterization of the polymers' microstructure is performed using 1D (^{1}H, ^{13}C, and DEPT-135) and 2D (heteronuclear single quantum coherence (HSQC), heteronuclear single quantum coherence−total correlation spectroscopy (HSQC−TOCSY), and heteronuclear multiple bond correlation (HMBC) NMR. On-line LC-NMR has also been employed in order to determine the presence of homopolymers in diblock samples. Finally, preliminary morphology studies have been performed using solid-state NMR.

Experimental Section

Materials. Commercially available hexamethylcyclotrisiloxane (Aldrich) was purified by melting and stirring over CaH_2 for ca. 12 h, followed by vacuum sublimation. *sec*-Butyllithium (1.3 M in hexane, Aldrich) was titrated using the Gilman double-titration method.[29] Allyl bromide, NaH, $(CH_3)_2$ClSiH (Aldirch), and the catalyst Pt−divinyltetramethyldisiloxane complex (3−3.5% Pt, Gelest) were all used as received. THF, DMF, styrene, and toluene were purified according to procedures described in the literature.[30]

Instrumentation. 1D and 2D NMR characterizations were performed on two spectrometers. ^{1}H, HSQC-gs, HSQC-TOCSY-gs, HMBC-gs, and COSY-gs were performed on a Bruker DMX400 spectrometer, using a 5 mm inverse probe. ^{13}C and DEPT-135 spectra were obtained using a Bruker AMX500 spectrometer.

LC separation of the polymer was performed using a conventional LC system, equipped with both a UV (wavelength

220 nm) detector and an evaporative light scattering detector (ELSD, Polymer Laboratories, Inc.). Reversed phase separation was done using a SUPLECOSIL C18 column (25 cm × 4.6 mm), with a solvent gradient of acetonitrile/THF from 80/20 to 20/80 in 40 min. The LC system is online with a Varian UNITY-INOVA 600 MHz NMR spectrometer, with a 60 μL triple-resonance flow probe, with stop-flow capabilities. A needle valve splitter immediately after the column splits the mobile phase between the two detectors, with 85−95% of the eluent going to the UV detector and subsequently the NMR flow probe; the remaining eluent goes to the ELSD. ^{1}H NMR analysis of the copolymer was performed, using pulse field gradient techniques to suppress signals from solvent and reaction byproducts.

Synthesis of BST and Hawker's Initiator. Compound **1** was synthesized according to the procedure described by Kobatake, Harwood, and Quirk.[19] For purification **1** was filtered over a column of silica gel and recrystillized from ethanol to obtain the product in 50% yield based on TEMPO (mp 72−73 °C). Compound **2** was synthesized according to the literature.[18,19] To ensure complete drying, **2** was dissolved in benzene, and rotary evaporated to remove the solvent. This procedure was repeated three times. The product was placed on a vacuum line to remove residual solvents. **2** was a pale yellow liquid, obtained in 87% yield.

Synthesis of Allyl Ether. Compound **2** was mixed with 4 equiv of NaH in DMF (total concentration 0.1 M of **2** in DMF). The solution was allowed to stir under N_2 for 1 h at room temperature. After 1 h, 6 equiv of allyl bromide was added dropwise via an addition funnel, and the solution was allowed to stir for 20 h at room temperature. The reaction mixture was diluted with H_2O, extracted with hexane, and dried over $MgSO_4$. A yellow, viscous liquid was obtained, which crystallized after purification by column chromatography (mp 32−33 °C). **3** was obtained in 73 and 78% product yields.

Synthesis of Hydride End-Capped PDMS. Hexamethylcyclotrisiloxane (D_3) was dissolved in THF (ca. 2.3 M), and the solution was stirred under N_2 until D_3 completely dissolved. *sec*-Butyllithium was then added via syringe to initiate polymerization. The reaction mixture was allowed to stir under N_2 at ca. 50 °C. To minimize backbiting and chain scrambling reactions, which broaden molecular weight distribution, the reaction was monitored by MALDI-ToF MS.[31−33] Polymerization was quenched with excess $(CH_3)_2ClSiH$ after 3 h. The reaction mixture was poured into an excess of acetonitrile to precipitate the polymer. The polymer (**4**) was recovered by decantation and placed on a vacuum line to remove residual solvents. A colorless, viscous oil was obtained on the average of ca. 80% yield based on D_3.

Hydrosilylation of Hydride End-Capped PDMS. Hydride end-capped PDMS (**4**) was dissolved in toluene (ca. 0.01 M solution) in a pressure bottle. To this, 1.25 equiv (based on the estimated moles of Si−H in **4**) of **3** were added, and the solution was stirred with a glass rod until **3** completely dissolved. Next, 2 drops (ca. 10 μL) of platinum catalyst (Pt−divinyltetramethyl disiloxane complex) were added to the pressure bottle. The bottle was sealed tightly and placed in an oil bath at ca. 50−60 °C for 24 h. Upon cooling, the solution was diluted with toluene and filtered over a plug of deactivated charcoal and Celite to remove any particulates and for decolorization. The polymer was then precipitated from toluene with methanol and decanted, and the recovered polymer was placed on a vacuum line to remove residual solvents. A viscous, slightly murky oil was obtained in ca. 55−60% yield.

Synthesis of PDMS-*b*-PS. A high-pressure reaction tube was charged with monomer and macroinitiator. Three freeze−dry cycles were performed to evacuate the reaction tube. Reaction tubes were then placed in a sand bath for 72 h at 130 °C. After 72 h, the viscous polymer slurry was dissolved in THF in order to remove it from the reaction tube. An aliquot of the polymer solution was taken to determine percent conversion by ^{1}H NMR. The polymer was precipitated from THF using a large excess of methanol, collected by decantation, and dried in vacuo. The average conversion was 94%.

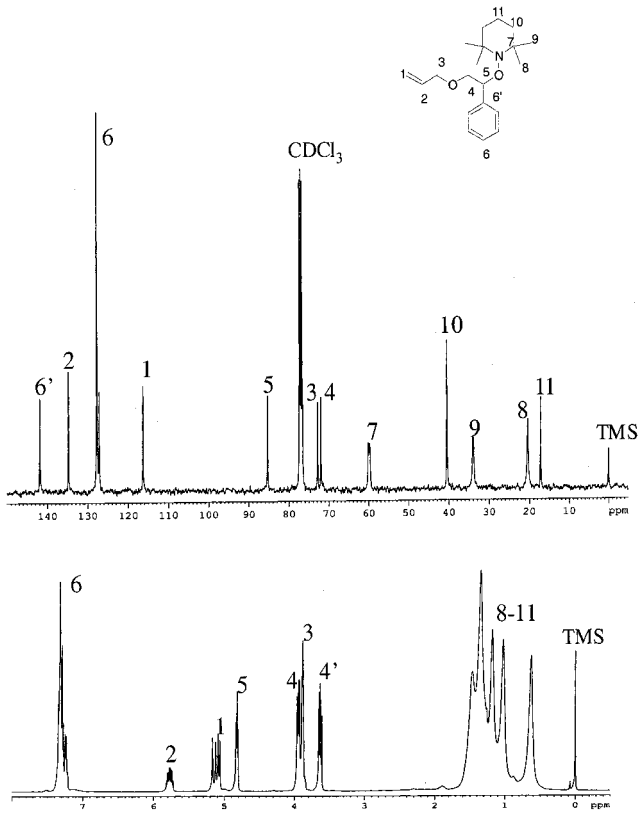

Figure 1. (a) ^{1}H and (b) ^{13}C NMR of allyl ether.

Results and Discussion

Allyl Ether. The functionality of the alkoxyamine **2** can be altered by reacting it with an allyl halide. The product is a difunctional alkoxyamine, capable of hydrosilylation and nitroxide-mediated radical polymerization.

The ^{1}H and ^{13}C spectra of **3** are illustrated in Figure 1. Identification of the proton and carbon moieties of this molecule was made using ^{1}H, ^{13}C, DEPT-135, and 2D HSQC-NMR. The broad multiplet, resonating at 0.5−1.7 ppm, is due to TEMPO. The line width of this signal is inversely proportional to the value of T_2, the spin−spin relaxation time, which is effected by motional averaging in a molecule. Lack of motional averaging causes T_2 to be short, resulting in dipolar broadening. Molecules with restricted motion (i.e., polymers, rigid solids) have short T_2 values, causing broad signals in the ^{1}H spectrum of the molecule. Hence, the broad signal in the spectrum of the allyl ether indicates that TEMPO is locked in a rigid conformation.

In the ^{13}C spectrum of **3**, note that the methyl carbons, 8 and 9, have different chemical shifts. This, again, alludes to the locked conformation of TEMPO. As seen with other six-membered cyclic systems (i.e., cyclohexane at low temperatures), the axial position experiences a slightly more shielded magnetic environment from the equatorial position, causing a difference in chemical shift. Molecular modeling of the allyl ether shows that TEMPO in its lowest energy state exists in a locked chair conformation. Also, carbons 8 and 9's proximity to the chiral benzylic carbon 5 attributes to the chemical shift difference. These factors cause a chemical shift difference of 13.66 ppm for carbons 8 and 9.

Hydride End-Capped PDMS. Anionic polymerization of hexamethylcyclotrisiloxane (D_3) has been exten-

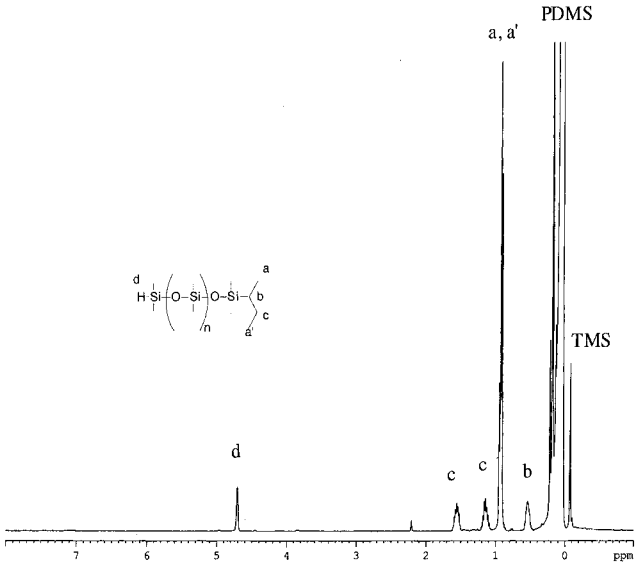

Figure 2. ^{1}H NMR of PDMS.

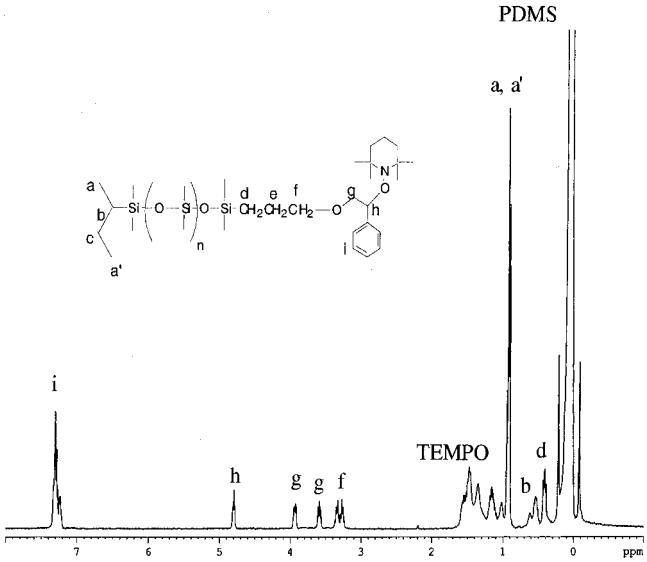

Figure 3. ^{1}H NMR of macroinitiator.

sively reviewed in the literature.[32−35] One of the well-known features of siloxane polymerization is the formation of cyclic byproducts, due to backbiting and chain redistribution reactions. The amount of cyclics formed increases with conversion, until equilibrium is reached.[32−35] This results in a broadened molecular weight distribution. To prevent this from occurring, the reaction was monitored by MALDI-ToF mass spectrometry.[31] MALDI-ToF analysis of polymer samples taken from the reaction at different time intervals (30 min, 3 h, 6 h, 9 h, and 24 h) showed that these side reactions can be kept to a minimum if the reaction is quenched at 3 h. Allowing polymerization to proceed for 3 h at ca. 50 °C resulted in 80% yield based on the amount of monomer used.

The ^{1}H NMR spectrum of **4** is illustrated in Figure 2. An intense peak resonating at 0.074 ppm represents the dimethyl protons on Si. The end groups, *sec*-butyl and Si−H, resonate at 0.51−1.59 and 4.72 ppm, respectively. The presence of the Si−H functional group was also confirmed by FT-IR, 2128.0 cm^{-1}. Comparing the integrals of the *sec*-butyl peaks and the Si−H peak results in a 9:1 ratio. This indicates that the majority of the polymer chains have the same end groups.

Macroinitiator. Hydrosilylation of hydride end-capped PDMS results in the macroinitiator **5**. The polymer was recovered by precipitation, leaving any unreacted allyl ether and/or nonpolymeric byproducts in solution. Confirmation of hydrosilylation was first made by FT-IR. The Si−H absorption band, at 2128.0 cm^{-1}, was absent from the spectrum of the macroinitiator upon completion of the reaction.

The ^{1}H NMR spectrum is illustrated in Figure 3. The presence of TEMPO is indicated by the characteristic broad signal, resonating at 0.4−1.6 ppm. Signals due to the *sec*-butyl end group lie underneath the broad TEMPO multiplet. Comparing the ^{1}H spectra of the allyl ether to that of the macroinitiator (see Figures 1a and 3**)**, one should notice the disappearance of the allylic proton peaks at 5.13 and 5.77 ppm, further indicating hydrosilylation. The CH_2 protons 3 have also shifted upfield to 3.3 ppm (f in Figure 3). Peaks corresponding to 4, 5, and 6 (g, h, and i in Figure 3) remain at roughly the same chemical shift. There is no indication of side reactions, such as α-addition, or unreacted hydride end-capped PDMS in the spectrum.

Table 1. Results of Hydride End-Capped PDMS and Macroinitiator

sample ID	[D_3/*s*-BuLi]	M_n (calc)	M_n (GPC)	M_w (GPC)	M_w/M_n (GPC)
PDMS (**4**)	16	3749	4606	5552	1.20
macroinitiator (**5**)	na	4066	4167	5094	1.22

Table 2. Results of Diblock Synthesis

sample ID	[Sty/**4**] (molar ratio)	M_n (calc)	M_n (GPC)	M_w (GPC)	M_w/M_n (GPC)
DB-1	154	20 330	19 754	26 645	1.35
DB-2	74	11 885	10 378	13 156	1.27
DB-3	50	9 369	9 495	12 242	1.29

PDMS-*b*-PS. Diblocks were formed by bulk stable free radical polymerization of styrene, using the macroinitiator as the initiator and nitroxide source. Table 2 summarizes the GPC results of the diblocks. For each diblock, approximately equal amounts of macroinitiator, **4**, were used, varying the amount of styrene monomer. Comparing the M_n values for diblocks 1, 2, and 3, M_n increased with an increasing amount of monomer charged to the reaction tube. This indicates that the reaction is behaving in a living manor, with styrene polymerization initiated by the macroinitiator. For diblocks 1 and 3, M_n values determined from GPC are less than 5% different from the calculated M_n's. Diblock 2 shows a slight deviation from the calculated M_n, but results are still comparable to the theoretical value. GPC elution curves for these samples show unimodal distributions, with the elution curve of diblock 1 having a slight shoulder at the high molecular weight region. This indicates some inhomogeneity in diblock 1, resulting from autopolymerization of styrene, or diblocks very heavy in styrene content (see LC-NMR Characterization). For all three samples, $M_w/M_n \leq 1.35$, which is below the theoretical limiting polydispersity of 1.5 for a conventional free-radical polymerization process. With only a slight increase in the polydispersity of the diblocks as compare to the macroinitiator, one may assume that the PS block is nearly monodispersed. However, it is realized that GPC (based on PS standards) cannot be used to determine the polydispersity for each individual block. Other techniques such as LCCC or MALDI-ToF MS must be used to evaluate these properties.

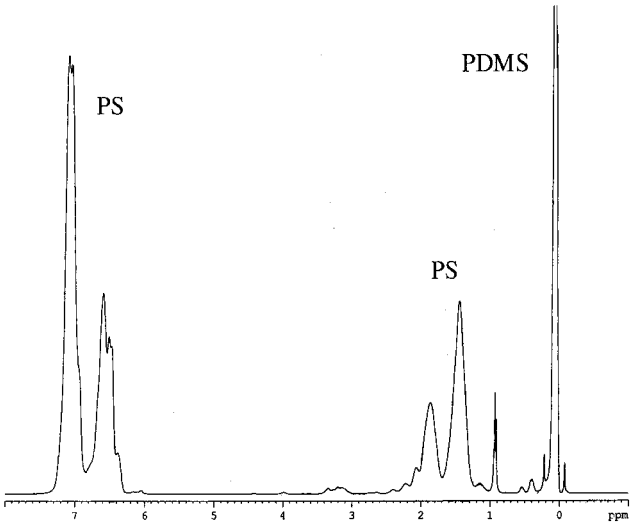

Figure 4. ^{1}H NMR of PDMS-*b*-PS.

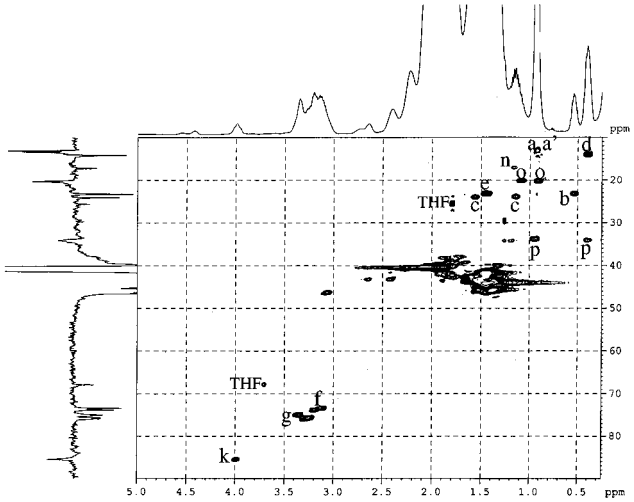

Figure 5. HSQC NMR of PDMS-*b*-PS.

NMR Characterization. ^{1}H NMR verifies gross monomer composition. In Figure 4, the sharp peak resonating at 0.074 ppm represents the PDMS block of the polymer. Broad peaks at 1.2−2.5 ppm (aliphatic backbone) and 6.0−7.5 ppm (aromatic side chain) represent the PS block. Peaks due to the polymer microstructure are observed between 0.3 and 5.0 ppm.

Microstructure characterization is carried out using multidimensional NMR techniques. First, $^1J_{CH}$ correlations are established by HSQC. A ^{1}H subspectrum of the aliphatic region is illustrated on the *x*-axis of the HSQC spectrum (Figure 5). DEPT-135 was used to determine the nature of each carbon moiety, and this subspectrum is illustrated on the *y*-axis. Cross-peaks a and a′ correspond to methyl carbons at 13.03 and 13.35 ppm. The cross-peaks d and n correspond to methylene peaks at 14.09 and 17.16 ppm. Methyl carbon peaks at 20.24 and 33.90 ppm, o and p, are assigned to two cross-peaks each. These cross-peaks indicate carbons with nonequivalent protons. The methylene peak c is also assigned to two cross-peaks, again indicating nonequivalent protons. Overlapping peaks b and e correspond to a methine and a methylene group with approximately the same chemical shift (23.29 ppm). In the region where the aliphatic PS signal occurs, there are three cross-peaks that do not correspond to the polymers backbone. These peaks are due to methylene

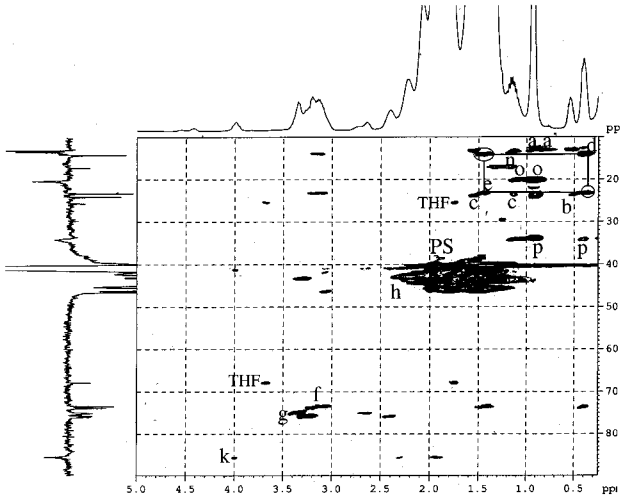

Figure 6. HSQC-TOCSY NMR of PDMS-*b*-PS.

or methine carbons neighboring a phenyl group; however, their exact identity could not be determined by HSQC. Cross-peaks f, g, and k correlate to methylene and methine carbons at 73.87, 78.99, and 85.55 ppm. On the basis of the chemical shift, these carbons are alkoxy in nature.

Next, connectivity between neighboring groups is established by HSQC−TOCSY. HSQC−TOCSY shows $^1J_{CH}$ ^{1}H−^{13}C correlation, along with ^{1}H−^{1}H correlations (TOCSY). In an HSQC−TOCSY spectrum, one observes the same cross-peaks from HSQC, with new cross-peaks arising due to TOCSY. Direct correlations between neighboring moieties can be determined by this technique, enabling further elucidation of the polymer microstructure.[36] Figure 6 illustrates the HSQC−TOCSY spectrum of the diblock. Connectivity is established by finding correlations between cross-peaks identified by HSQC to new cross-peaks due to TOCSY. For example, the methylene carbon d at 14.03 ppm has two cross-peaks: one present at 0.398 ppm seen in the HSQC spectrum and a new cross-peak at 1.45 ppm due to TOCSY. These cross-peaks correlate this carbon to its directly attached protons at 0.398 ppm and the neighboring methylene protons at 1.45 ppm. This same connectivity can be established by carbon e at 23.29 ppm, which also has cross-peaks at 0.398 and 1.45 ppm. Hence, carbons d and e are connected. Other connectivities, established in a similar fashion, are as follows: $^{a}CH_3-^{b}CH-^{c}CH_2-^{a'}CH_3$, representing the *sec*-butyl end group, and $^{d}CH_2-^{e}CH_2-^{f}CH_2-O$, representing part of the block junction. The methylene alkoxy carbon g shows signs of correlation with a cross-peak at around 2.4 ppm in the ^{1}H dimension. Connectivity between these moieties was confirmed by COSY, showing correlation between protons g and h. For TEMPO, the only correlation that can be detected by HSQC−TOCSY is between its methylene groups. From ^{13}C analysis of the allyl ether, methylene carbon 10 of TEMPO resonates in the same region as the aliphatic PS signal in the diblock. Hence, connectivity within TEMPO cannot be confirmed, due to the overlap of the aliphatic PS signal.

To confirm connectivity within TEMPO, HMBC was performed. HMBC was chosen, because it allows one to establish ^{1}H−^{13}C connectivity via multiple bond J_{CH}, even through nonpotonated heteroatoms. The HMBC spectrum is illustrated in Figure 7. In this 2D spectrum the ^{13}C spectrum is substituted for DEPT-135 in order to illustrate correlations with nonprotonated carbons.

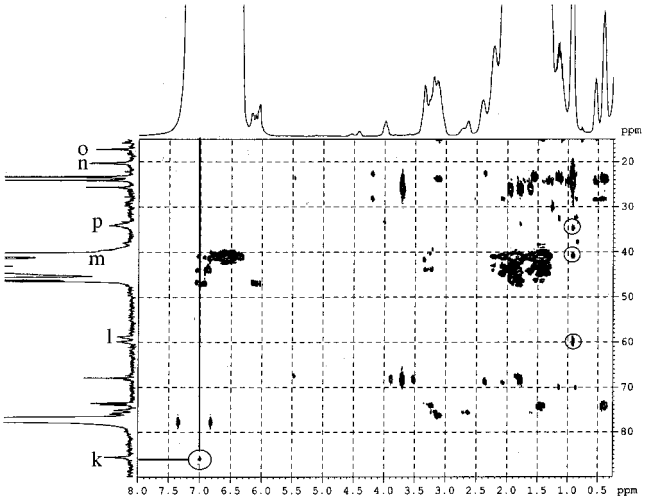

Figure 7. HMBC NMR of PDMS-*b*-PS.

In the HMBC spectrum, one observes cross-peaks corresponding to carbons l (quaternary carbon of TEMPO, absent from DEPT-135) and p around 59.0 and 33.9 ppm, respectively. Also, there is a cross-peak at 40.5 ppm in the ^{13}C dimension, corresponding to a carbon underneath the aliphatic PS signal, m. Cross-peaks l, m, and p occur at the same proton chemical shift as the methyl protons o (see Figure 5), establishing $^{2}J_{CH}$ and $^{3}J_{CH}$ connectivity between o with l, m, and p. Cross-peak k shows connectivity to aromatic protons, establishing its benzylic character. However, no connectivity between k and TEMPO is seen by HMBC. To observe $^{1}H-X$ correlation between the benzylic carbon k and any TEMPO moieties, J_{CH} would have to be detected through a minimum of four bonds ($^{4}J_{CH}$), exceeding the detection limits under the current acquisition parameters for this experiment. Despite the fact that connectivity between k and TEMPO was not established by HMBC, the ^{1}H chemical shift of TEMPO-bonded k proton, resonating at 3.9 ppm (see Figure 5), agrees with values reported in the literature.[37,38] Proton and carbon chemical shifts for the identified groups are illustrated in Figure 8 and summarized in Table 3.

Now that the polymer's microstructure has been verified, the relative abundance of each end group must be discussed. Comparing the integral of carbon peak n of TEMPO to that of c of the *sec*-butyl group, the ratio is approximately 2:3. If all polymer chains contain the TEMPO end group, the relative ratio should be 2:1. The low abundance of TEMPO as compared to the *sec*-butyl end group indicates that all polymer chains are not capped with TEMPO. It has been reported that other end groups may result during NMRP of styrene due to hydrogen-transfer reactions.[39] Hydrogen transfer results in an unsaturated $-CH{=}CHPh$ end group from disproportionation and a saturated $-CH_2-CH_2Ph$ end group from oxidation of the benzylic radical with hydroxy TEMPO, formed during propagation. There is no evidence of the unsaturated end group from NMR analysis. There is, however, some evidence of aliphatic protons from COSY. Unfortunately, their exact identity and connectivity were not determined.

LC-NMR Characterization. Autopolymerization of styrene is known to occur during NMRP.[39−41] To scout for homopolymer PS and unreacted PDMS homopolymer in the sample, LC-NMR was performed. Figure 9

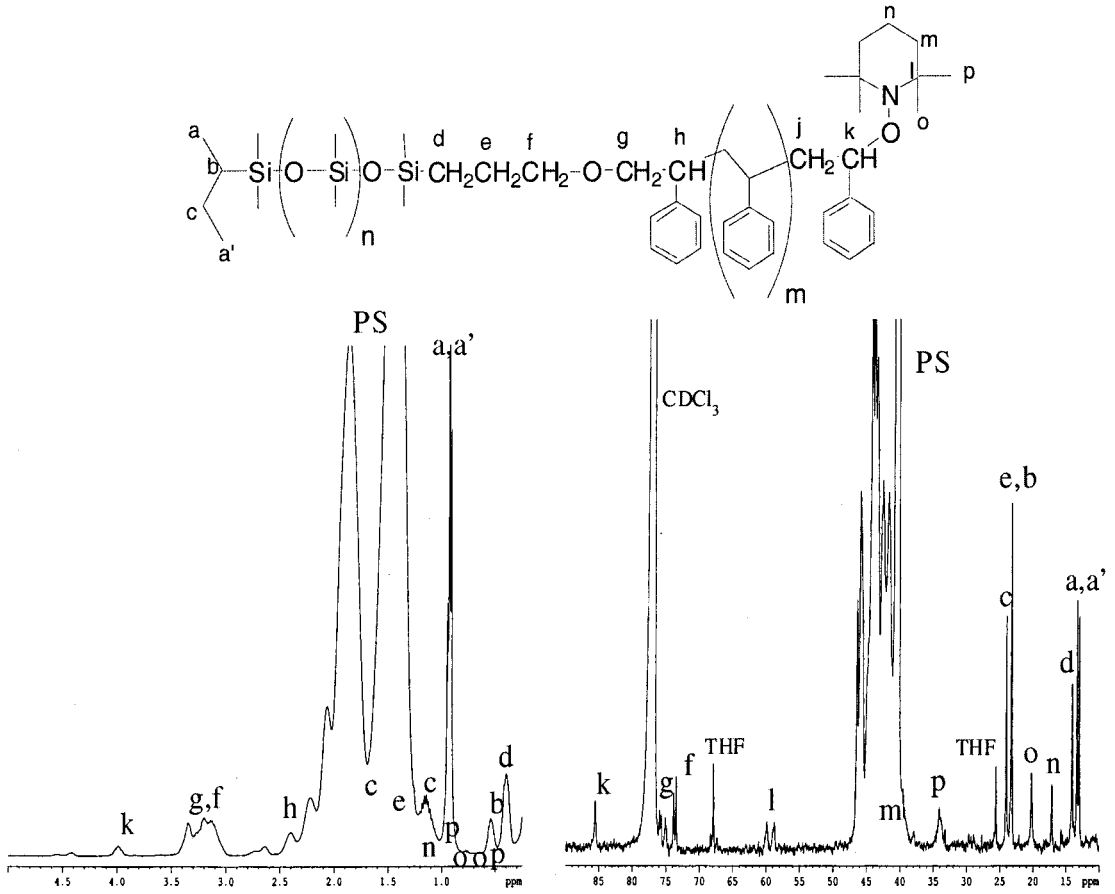

Figure 8. ^{1}H and ^{13}C subspectra of PDMS-*b*-PS.

Table 3. ^{13}C and ^{1}H Chemical Shifts, Determined by 1D and 2D NMR

sec-butyl end group			block junction			TEMPO end group		
position	δ ^{13}C in ppm	$\delta^{1}H$ in ppm	position	δ ^{13}C in ppm	δ ^{1}H in ppm	position	δ ^{13}C in ppm	δ ^{1}H in ppm
a	13.03	0.948	d	14.09	0.398	j	n.i.	n.i.
a′	13.35	0.948	e	23.29	1.451	k	85.55	3.998
b	23.29	0.542	f	73.57	3.159	l	58.76, 59.84	NA
c	24.04	1.143, 1.560	g	75.80	3.260	m	40.48	n.i.
			h	n.i.	2.401	n	17.16	1.158
						o	20.24	1.083
								0.913
						p	33.90	0.937
								0.401

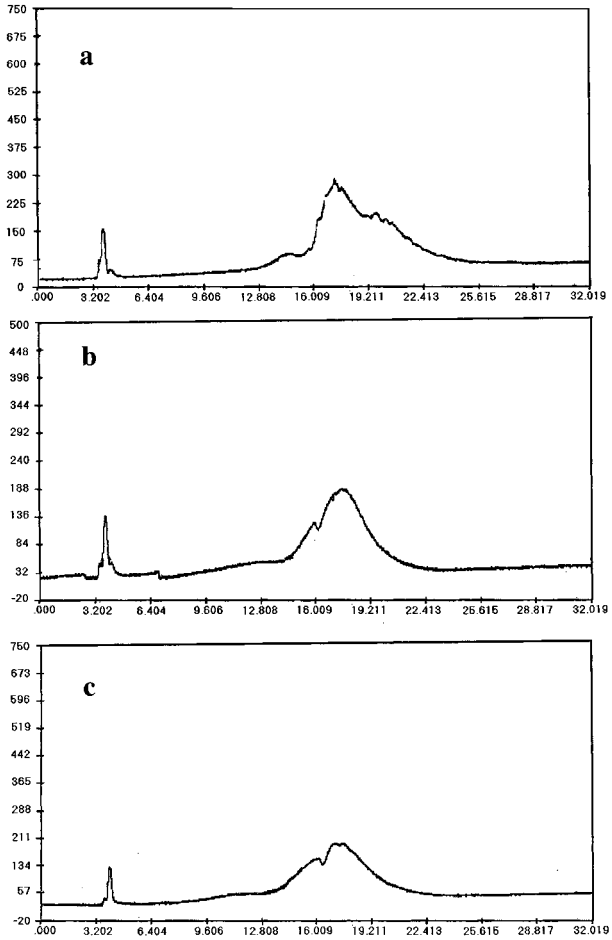

Figure 9. LC of diblocks (a) **DB-1**, (b) **DB-2**, and (c) **DB-3**.

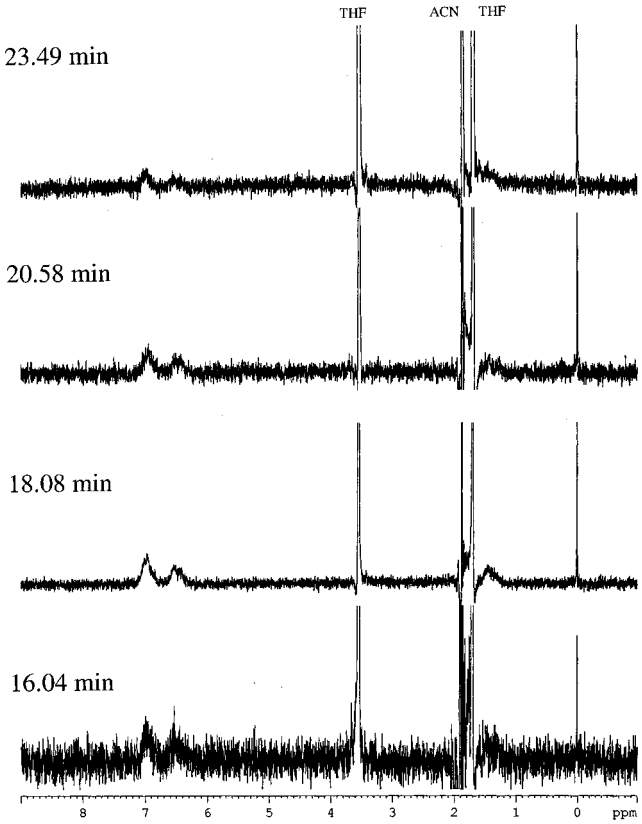

Figure 10. ^{1}H NMR results from LC-NMR of **DB-1**.

illustrates LC (UV detector) data for diblocks 1, 2, and 3 (**DB-1**, **DB-2**, and **DB-3**). In each chromatograph, there is a broad peak, with some regions of inhomogeneity. Figure 10 illustrates ^{1}H NMR results for diblock 1 between 16.0 and 23.0 min. At each retention time, the corresponding spectrum illustrates a sharp PDMS peak around 0.1 ppm and a broad PS peak at 6.0−7.5 ppm, proving that block copolymer exist between these retention times. In both parts b and c of Figure 10, there exist a shoulder just below 16.0 min that is inconsistent with the main peak. ^{1}H NMR data for this region are not shown; however, results for this region indicate that this shoulder is block copolymer. Also, LC analysis of polystyrene standards under the same conditions showed that polystyrene elutes between 7.0 and 14.0 min. Hence, no homopolymer polystyrene is detected in any of the samples. These results indicate that any autopolymerization of styrene that may have occurred during copolymer synthesis in minimal. PDMS homopolymer was detected for one of the samples, **DB-3**. In Figure 11, LC analysis using an ELSD detector showed a peak at 26.8 min. The lack of UV response at this retention time indicates that this peak is due to homopolymer PDMS. This is confirmed by ^{1}H NMR, having the characteristic PDMS peak around 0.1 ppm. Compared to the ELSD response of the diblock, this peak is very minor. The minute presence of PDMS homopolymer may be due to incomplete reaction of the hydride-terminated PDMS. Despite the detection of trace amounts of PDMS in **DB-3**, it can be concluded that these materials are nearly free of homopolymers.

Although LC-NMR results show that these diblocks were nearly free of homopolymers, there was some inhomogeneity in these samples. These differences are further indicated by the change in the relative intensity of the PS and PDMS peaks with retention time. For **DB-1**, the relative molar ratio of PS to PDMS was estimated from integration of peaks in Figure 10. Based on integration, the molar ratio of PS:PDMS varied from 3:1 to 6:1. The maximum ratio was approximately 6:1 at 18.08 min, the highest intensity region of the chromatograph. The minimum PS:PDMS molar ratios were

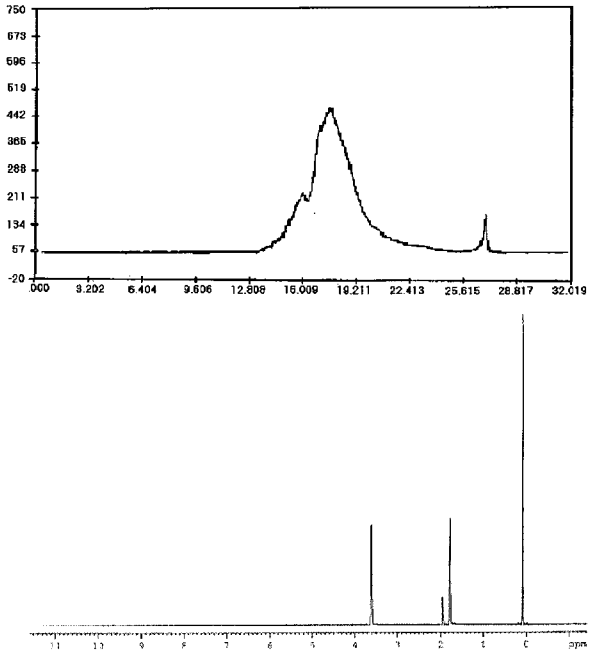

Figure 11. (a) LC (ELSD) for **DB-3**. (b) ^{1}H spectrum at retention time of 26.9 min.

4:1 and 3:1 at 16.04 and 20.58 min, respectively. ^{1}H NMR results for **DB-2** and **DB-3** also indicated a change in relative intensity. Ratios of PS:PDMS varied from 5:1 to 1:1 in these samples, with the molar ratios being approximately 2:1 in the highest intensity region of the chromatograph for both samples. The shoulder just below 16.0 min has the maximum ratio of PS to PDMS, corresponding to 5:1 and 4:1 in **DB-2** and **DB-3**, respectively. These results indicate that regions of inhomogeneity in the chromatographs are due to diblocks with varying PS to PDMS molar ratios.

Solid-State NMR. One of the aims of synthesizing PDMS-*b*-PS by this two-step process is to use this technique to make diblocks with specific morphologies. To obtain a specific morphology (lamellar, cylinders, spheres, bicontinueous), the system of interest must exhibit phase segregation between the two blocks. Considering the drastically different T_g's of PDMS (T_g −125 °C) and PS (T_g 104 °C, depending on molecular weight), one would certainly expect diblocks of these materials to be phase segregated. To verify this, a WISE solid-state NMR (cphp-TOSS WISE) experiment was performed. This is a 2D solid-state NMR experiment, which correlates carbon and proton chemical shifts. Using the WISE experiment, one may distinguish between carbons attached to protons in a rigid environment vs those in a mobile environment.[42] As explained previously, materials with restricted motion have broad protons signals, while mobile molecules have relatively sharp signals. Figure 12 illustrates the WISE spectrum of **DB-1**. The sharp signal in the proton dimension (*y*-axis) is correlated with the PDMS carbon signal (*x*-axis), while the broad line width correlates to the PS carbon signals. These correlations indicate that there exists a hard and soft segment of the diblock, verifying phase-segregated morphology.

TEM analysis of these materials was attempted but unsuccessful due to difficulty in casting films from common solvents.[43] Higher molecular weight materials, with the molecular weight of each component above its entanglement molecular weight, must be synthesized

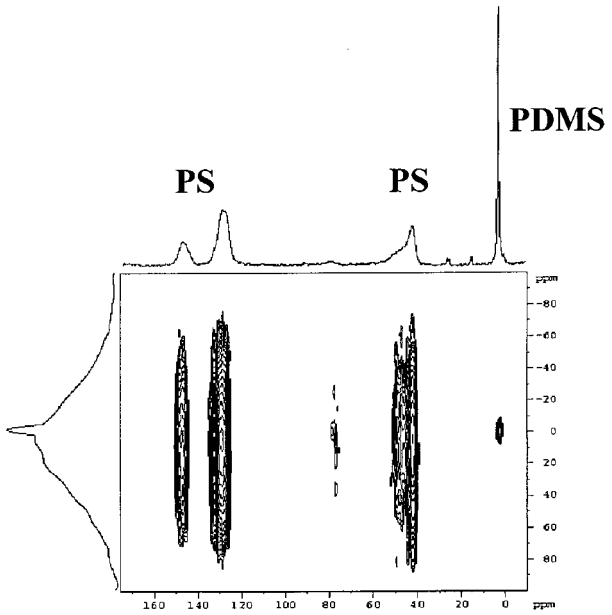

Figure 12. Solid-state NMR (cphp TOSS−WISE) spectra of **DB-1**.

in order to determine the specific morphology of the diblocks.

Conclusion

PDMS-*b*-PS copolymers have been synthesized by anionic polymerization and nitroxide-mediated radical polymerization. Molecular weights determined by GPC agreed well with calculated values, yielding relatively low polydispersities. Microstructure characterization verified the incorporation of the *sec*-butyl and TEMPO end groups and the block junction. LC-NMR analysis showed that nearly homopolymer free diblock could be obtained by this method. Solid-state NMR analysis verified the phase-segregated morphology, typical of PDMS/PS copolymers. From the information presented, one may conclude that this is a viable technique for synthesizing PDMS-*b*-PS copolymers. Diblocks of a specific architecture, with reasonable control over the molecular weight and polydispersity, can be obtained without the use of high-vacuum techniques and special equipment necessary for anionic polymerization. However, one may question the efficiency of this method since multiple steps are involved. A more efficient mode of polymerization is currently being explored. This method involves synthesizing TEMPO end-capped PDMS using a lithium alkoxide of the Hawker initiator, followed by NMRP of PS. Diblocks formed by this route will be discussed in a future publication.

Acknowledgment. Special thanks to Rohm and Haas Co. for the support of this research through the Minority Graduate Research Internship Program (MGRIP). A.M.M. thanks Dr. Jian Wu and Dr. Dan Dohmeier of the Rohm and Haas Co. for discussions and applications of LC-NMR and preparative GPC.

References and Notes

(1) (a) Yilgor, I.; Mcgrath, J. E. In *Polysiloxane Copolymers/ Anionic Polymerization*; Yilgor, I., McGrath, J. E., Eds.; Advances in Polymer Science 86; Springer-Verlag: New York, 1988; pp 1−86. (b) Mark, J. In *Silicon-Based Polymer Science: A Comprehensive Resource*; Zeigler, J. M., Fearon, F. W., Gordon, Eds.; Advances in Chemistry Series 224;

American Chemical Society: Washington, DC; pp 47−70. (c) Chojnowski, J. In *Siloxane Polymers*; Clarson, S. J., Semlyen, J. A., Eds.; Polymer Science and Technology Series; PTR Prentice Hall: Engelwood Cliffs, NJ, 1993; pp 1−62.
(2) (a) Yokota, M.; Goshima, T.; Fujioka, S. US Patent 4,632,-968, 1986. (b) Falender, J. R.; Lindsey, S. E.; Ward, A. H.; Kendrick, T. C. US Patent 3,975,455, 1976. (c) Mann, R. H.; Sun, E. I.; Plamthottam, S. S.; Newing, C. W. US Patent 5,-728,469, 1998. (d) Pacansky, T. J.; Amidon, A. B. US Patent 4,218,514, 1980. (e) Gabor, A. H.; Ober, C. K. In *Microelectronics Technology. Polymers for Advanced Imaging and Packaging*; ACS Symposium Series 614; American Chemical Society: Washington, DC, 281.
(3) (a) DeSimone, J. M.; Jones, T. A.; Shaffer, K. A. *Macromolecules* **1996**, *29*, 2704. (b) DeSimone, J. M.; Betts, D. E.; Canelas, D. A. *Macromolecules* **1996**, *29*, 2818. (c) DeSimone, J. M.; Canelas, D. A. *Macromolecules* **1997**, *30*, 5673.
(4) Saam, J. C.; Gordon, D. J.; Lindsey, S. *Macromolecules* **1970**, *3*, 1.
(5) Zillion, J. G.; Roovers, E. L.; Bywater, S. *Macromolecules* **1975**, *8*, 573.
(6) Bajaj, P.; Varshney, S. K.; Misra, A. *J. Polym. Sci., Polym. Chem. Ed.* **1980**, *18*, 295.
(7) Dems, A.; Strobin, C. *Makromol. Chem.* **1991**, *192*, 2521.
(8) Chu, J. H.; Rangarajan, P.; Adams, J. L.; Register, R. A. *Polymer* **1995**, *36*, 1569.
(9) Molenberg, A.; Möller, M.; Pieper, T. *Macromol. Chem. Phys.* **1998**, *199*, 299.
(10) Rosati, D.; Perrin, M.; Navard, P. *Macromolecules* **1993**, *31*, 4301.
(11) Bellas, V.; Iatrou, H.; Hadjichristidis, N. *Marcromolecules* **2000**, *33*, 6993.
(12) Morton, M.; Fetters, L. J. *Rubber Chem. Technol.* **1975**, *48*, 359.
(13) Hadjichristidis, N.; Iatrou, H.; Pispas, S.; Pitsikalis, M. *J. Polym. Sci., Part A: Polym. Chem.* **2000**, *38*, 3211.
(14) Matyjaszewski, K.; Teodorescu, M.; Acar, M. H.; et al. *Macromol. Symp.* **2000**, *157*, 183.
(15) Matyjaszewski, K., Ed. *Controlled Radical Polymerization*; ACS Symposium Series 685; American Chemical Society: Washington, DC, 1998.
(16) Moad, G.; Rizzardo, E.; Solomon, D. H. *Macromolecules* **1982**, *15*, 909.
(17) Georges, M. K.; Veregin, R. P. N.; Daimon, K. In *Controlled Radical Polymerization*; Matyjaszewski, K., Ed.; ACS Symposium Series 685; American Chemical Society: Washington, DC, 1998; pp 170−179.
(18) Hawker, C. J.; Hedrick, J. L. *Macromolecules* **1995**, *28*, 2993.
(19) Kobatake, S.; Harwood, H. J.; Quirk, R. P. *Macromolecules* **1997**, *30*, 4238.
(20) Kobatake, S.; Harwood, H. J.; Quirk, R. P. *Macromolecules* **1998**, *31*, 3735.
(21) Puts, R. D.; Sogah, D. Y. *Macromolecules* **1996**, *30*, 7050.
(22) Malmström, E. E.; Hawker, J. *Macromol. Chem. Phys.* **1998**, *199*, 923.
(23) Miura, Y.; Hirota, K.; Moto, H.; Yamada, B. *Macromolecules* **1999**, *32*, 8356.
(24) Tsoukatos, T.; Pispas, S.; Hadjichristidis, N. *Macromolecules* **2000**, *33*, 9504.
(25) Hua, F. J.; Yang, Y. L. *Polymer* **2001**, *42*, 1361.
(26) Yoshida, E.; Tanimoto, S. *Macromolecules* **1997**, *30*, 4018.
(27) Miura, Y.; Hirota, K.; Moto, H.; Yamada, B. *Macromolecules* **1999**, *32*, 8356.
(28) Matyjaszewski, K.; Miller, P. J.; Nakagawa, Y. *Polymer* **1998**, *39*, 5163.
(29) Gilman, H.; Carledge, F. K. *J. Organomet. Chem.* **1964**, *2*, 447.
(30) Armarego, W. L. F.; Perrin, D. D. *Purification of Laboratory Chemicals*, 4th ed.; Butterworth-Heinemann: Oxford, 1996.
(31) Pollack, S. K.; Singer, D. U.; Morgan, A. M. *Polym. Prepr. (Am. Chem. Soc., Div. Polym. Chem.)* **2000**, *41* (1), 631.
(32) (a) Yilgor, I.; McGrath, J. E. In *Polysiloxane Copolymers/ Anionic Polymerization*; Yilgor, I., McGrath, J. E., Eds.; Advances in Polymer Science 86; Springer-Verlag: New York, 1988; pp 1−86. (b) Mark, J. In *Silicon-Based Polymer Science: A Comprehensive Resource*; Zeigler, J. M., Fearon, F. W. G., Eds.; Advances in Chemistry Series 224; American Chemical Society: Washington, DC; pp 47−70. (c) Chojnowski, J. In *Siloxane Polymers*; Clarson, S. J., Semlyen, J. A., Eds.; Polymer Science and Technology Series; PTR Prentice Hall: Engelwood Cliffs, NJ, 1993; pp 1−62.
(33) Boileau, S. In *Ring Opening Polymerization*; McGrath, J. E., Ed.; American Chemical Society: Washington, DC, 1985; pp 23−35.
(34) Lee, C. L.; Johannson, O. K. *Polym. Prepr. (Am. Chem. Soc., Div. Polym. Chem.)* **1969**, *10* (2), 1361.
(35) Veith, C. A.; Cohen, R. E. *Makromol. Chem., Macromol. Symp.* **1991**, *42*, 241.
(36) Beshah, K. *Macromolecules* **1992**, *25*, 5597.
(37) Chong, K.; Rizzardo, E.; Solomon, D. H. *J. Am. Chem. Soc.* **1983**, *105*, 7761.
(38) Komber, H.; Gruner, M.; Malz, H. *Macromol. Rapid Commun.* **1998**, *19*, 83.
(39) He, J.; Li, L.; Yang, Y. *Macromolecules* **2000**, *33*, 2286.
(40) Georges, M. K.; Veregin, R. N. P.; Kazmaier, P. M. *Trends Polym. Sci.* **1994**, *2*, 66.
(41) Devonport, W.; Michalak, L.; Malmström, E.; Mate, M.; Kurdi, B.; Hawker, C. J.; Barclay, G. G.; Sinta, R. *Macromolecules* **1997**, *30*, 1929 and literature cited therein.
(42) Bovey, F. A.; Mirau *NMR of Polymers*; Academic Press: San Diego, CA, 1996.
(43) Krause, S.; Iskandar, M.; Iqbal, M. *Macromolecules* **1982**, *15*, 105.

MA0114178